



## An injectable drug delivery platform for sustained combination therapy

M. Douglas Baumann<sup>a,b,c,1</sup>, Catherine E. Kang<sup>a,b,c,1</sup>, Jason C. Stanwick<sup>a,c,1</sup>, Yuanfei Wang<sup>a,b,c,1</sup>, Howard Kim<sup>c,d,1</sup>, Yakov Lapitsky<sup>a,1</sup>, Molly S. Shoichet<sup>a,b,c,d,e,\*</sup>

<sup>a</sup> Department of Chemical Engineering and Applied Chemistry, University of Toronto, 200 College Street, Toronto, ON, Canada M5S 3E5

<sup>b</sup> Institute of Biomaterials and Biomedical Engineering, 164 College Street, Toronto, ON, Canada M5S 3G9

<sup>c</sup> Terrence Donnelly Center for Cellular and Biomolecular Research, 160 College Street, Toronto, ON, Canada M5S 3E1

<sup>d</sup> Institute of Medical Science, University of Toronto, 1 King's College Circle, Toronto, ON, Canada M5S 1A8

<sup>e</sup> Department of Chemistry, University of Toronto, 80 St. George Street, Toronto, ON, Canada M5S 3H6

### ARTICLE INFO

#### Article history:

Received 22 April 2009

Accepted 6 May 2009

Available online 12 May 2009

#### Keywords:

Spinal cord injury

Drug delivery

Hydrogel

Nanoparticles

Combination therapy

### ABSTRACT

We report the development of a series of physical hydrogel blends composed of hyaluronan (HA) and methyl cellulose (MC) designed for independent delivery of one or more drugs, from 1 to 28 days, for ultimate application in spinal cord injury repair strategies. To achieve a diversity of release profiles we exploit the combination of fast diffusion-controlled release of dissolved solutes from the HAMC itself and slow drug release from poly(lactide-co-glycolide) particles dispersed within the gel. Delivery from the composite hydrogels was demonstrated using the neuroprotective molecules NBQX and FGF-2, which were released for 1 and 4 days, respectively; the neuroregenerative molecules dbcAMP and EGF, and proteins  $\alpha$ -chymotrypsin and IgG, which were released for 28 days.  $\alpha$ -chymotrypsin and IgG were selected as model proteins for the clinically relevant neurotrophin-3 and anti-NogoA. Particle loaded hydrogels were significantly more stable than HAMC alone and drug release was longer and more linear than from particles alone. The composite hydrogels are minimally swelling and injectable through a 30 gauge/200  $\mu$ m inner diameter needle at particle loads up to 15 wt.% and particle diameters up to 15  $\mu$ m.

© 2009 Elsevier B.V. All rights reserved.

### 1. Introduction

About 11,000 new cases of traumatic spinal cord injury (SCI) are reported in the United States annually, primarily affecting young adults [1]. A majority of these cases are compression injuries wherein the cord is bruised under displacement of the spinal column, resulting in formation of a cystic cavity in the days after injury. As tissue degenerates, the degree of paralysis increases, causing further permanent loss of motor control and sensory perception. For this reason compression injuries are normally described as occurring in two stages, the immediate primary injury and subsequent secondary injury. Various treatment strategies are being developed with a view of limiting degeneration after the primary injury and/or promoting regeneration after secondary injury. Currently, however, there is no standard clinical treatment, other than application of methylprednisolone, the efficacy of which is still debated [2,3].

Therapies designed to enhance cell survival during the trauma of secondary injury are focused on the hours to days following the primary injury and seek to limit vascular damage, excitotoxicity, and the inflammatory response around the injury site [4]. Neuroprotective strategies target one or more of these mechanisms with the goal of minimizing the death of motor and sensory neurons. For example, methylprednisolone targets acute inflammation and inhibits lipid peroxidation [5], while the sodium channel antagonist NBQX minimizes excitotoxicity [6] and nimodipine limits vasospasm [7]. Neuroregenerative therapies enhance axonal outgrowth by either direct action or suppression of the inhibitory environment after injury. For example, numerous neurotrophins stimulate proliferation and regeneration, including: nerve growth factor [8], brain derived neurotrophic factor [9], epidermal growth factor (EGF) [10] and basic fibroblast growth factor (FGF-2) [11]. FGF-2 has also been reported to prevent neuronal cell death [12,13] and promote angiogenesis [14]. The family of antibodies targeting NogoA [15], rho kinase inhibitors [16] and cyclic AMP [17] are well known anti-inhibitory molecules that act by blocking or overriding the inhibitory environment present post-injury. These molecules are often delivered for extended periods, ranging from 7–28 days.

Whether neuroprotective or neuroregenerative, delivery is limited to local strategies as most molecules are unable to cross the blood-spinal cord barrier, confounding systemic delivery. Current local delivery strategies are inadequate: bolus delivery often results in rapid

\* Corresponding author. Terrence Donnelly Center for Cellular and Biomolecular Research, 514-160 College Street, Toronto, Ontario, Canada M5S 3E1. Tel.: +1 416 978 1460; fax: +1 416 978 4317.

E-mail addresses: [douglas.baumann@utoronto.ca](mailto:douglas.baumann@utoronto.ca) (M.D. Baumann), [catherine.kang@utoronto.ca](mailto:catherine.kang@utoronto.ca) (C.E. Kang), [jason.stanwick@utoronto.ca](mailto:jason.stanwick@utoronto.ca) (J.C. Stanwick), [yuanfei.wang@utoronto.ca](mailto:yuanfei.wang@utoronto.ca) (Y. Wang), [howard.kim@utoronto.ca](mailto:howard.kim@utoronto.ca) (H. Kim), [yakov.lapitsky@utoronto.ca](mailto:yakov.lapitsky@utoronto.ca) (Y. Lapitsky), [molly.shoichet@utoronto.ca](mailto:molly.shoichet@utoronto.ca) (M.S. Shoichet).

<sup>1</sup> Tel.: +1 416 978 0352.

clearance due to cerebrospinal fluid flow in the intrathecal space [18,19], whereas the indwelling catheter/external pump is associated with scarring and infection [20]. With a view toward developing a minimally-invasive drug delivery system that would provide sustained, local release of factors, we previously designed a novel delivery paradigm in which a drug loaded thermo-sensitive hydrogel is injected intrathecally and remains localized at the site of injection, delivering the drug load to the spinal cord [21] and then biodegrading. In this manner the hydrogel provides a platform for localized release over the life of the material. Fig. 1 shows that intrathecal injection bypasses the dura and arachnoid mater and limits convective drug redistribution from CSF flow, all barriers that negatively impact epidural delivery [22]. The procedure is minimally invasive when performed in conjunction with surgical decompression, a widely applied procedure in the management of acute SCI [23,24]. We subsequently developed a biocompatible and biodegradable blend of 2 wt.% hyaluronan and 7 wt.% methyl cellulose (2:7 HMC) for this application [25]. The role of MC is to form a physical hydrogel through hydrophobic junctions [26] and HA to increase solution viscosity and to enhance MC gel strength at lower temperatures through the salting out effect. Additionally, based on reports of the anti-inflammatory action of HA [27], this component is likely responsible for the beneficial, anti-inflammatory effect of 2:7 HMC in a compression model of SCI [25]. 2:7 HMC was found to degrade within 4–7 days *in vivo*, making it well suited for neuroprotective delivery strategies but unsuitable for drug delivery over the 2–4 weeks necessary for regenerative strategies [28]. Accordingly, these injectable hydrogels were used to deliver erythropoietin [28], as well as EGF and FGF-2 *via* simple diffusion [29]. For soluble molecules, the release profile is determined principally by diffusivity and occurs within 24 h due to the short diffusive path length *in vivo* [29].

Here we report the next generation HMC that provides longer term release suitable for combination neuroregenerative and neuroprotective strategies. We formulated high molecular weight blends of HA and MC (HMW HMC) which remain injectable and are stable for more than 28 days *in vitro*. To achieve longer-term release profiles, we dispersed formulations of drug loaded poly(lactic-co-glycolic acid) (PLGA) nano- and microparticles in the HMW HMC gel. Use of the drug delivery platform is demonstrated using six therapeutic molecules or models thereof, shown in Table 1, for periods between 1 and 28 days. This contribution demonstrates the composite HMW HMC hydrogel is a flexible, localized drug delivery platform for the

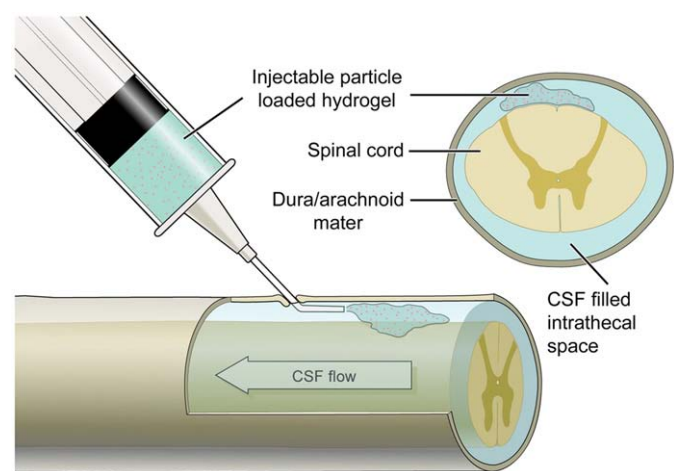


**Fig. 1.** An intrathecal drug delivery system. The composite hydrogel is injected intrathecally at the site of injury and remains localized between the arachnoid and pia mater, releasing the drug load into the spinal cord. Image copyright (2005) by Michael Corrin.

**Table 1**  
Molecules released from HMW HMC.

Molecule (model)	Molecular weight (kg/mol)	Neuro-protective	Neuro-regenerative	Desired treatment term
NBQX	0.336	*		days
dbcAMP	0.469		*	weeks
EGF	6.2		*	weeks
FGF-2	17	*	*	days
Neurotrophin-3 ( $\alpha$ -Chymotrypsin)	29 (25)		*	weeks
Anti-NogoA (IgG)	150 (150)		*	weeks

evaluation of therapies targeting protection and repair of the injured spinal cord.

## 2. Materials and methods

### 2.1. Materials

Recombinant human basic fibroblast growth factor (FGF-2, >95 wt.%) was purchased from Biovision (Santa Clara, USA). 2,3-Dioxo-6-nitro-1,2,3,4-tetrahydrobenzo[f]quinoxaline-7-sulfonamide disodium salt (sodium NBQX, >98 wt.%) was purchased from A.G. Scientific (San Diego, USA).  $\alpha$ -Chymotrypsin (type II from bovine pancreas), human IgG, and N<sup>6</sup>,2'-O-dibutyryl adenosine 3',5'-cyclic monophosphate sodium salt (dbcAMP) were purchased from Sigma-Aldrich (Oakville, CA). Recombinant human epidermal growth factor (EGF) was purchased from Peptrotech (Rocky Hill, USA).

Sodium hyaluronate of 1700 kg/mol was purchased from FMC Biopolymer (Sandvika, Norway) and of 2600 kg/mol from Lifecore (Chaska, USA). Methyl cellulose of 300 kg/mol was purchased from Shin-Etsu (Tokyo, Japan). Poly(DL-lactic-co-glycolic acid) 50:50 of inherent viscosity 0.15–0.25 dL/g and methyl cellulose (13 kg/mol) were purchased from Sigma-Aldrich. Poly(DL-lactic-co-glycolic acid) 50:50 of inherent viscosity 0.20 dL/g and 0.37 dL/g were purchased from Durect (Cupertino, USA). Poly(vinyl alcohol), 6 kg/mol and 80% mol hydrolyzed, was purchased from Polysciences Inc. (Warrington, USA). Polystyrene (220 nm, 510 nm, 830 nm, 3.09  $\mu$ m, 15.5  $\mu$ m) and poly(acrylic acid) (60 nm) particles were received as suspensions in water from Bangs Laboratories (Fishers, USA), scrubbed of surfactant by exposure to cation exchange resin (Amberlyst-15, Sigma-Aldrich), neutralized with 1M NaOH and lyophilized (Labconco, Kansas City, USA) prior to use.

HPLC grade dichloromethane (DCM) and dimethyl sulfoxide (DMSO) were supplied by Caledon Labs (Georgetown, CA). All buffers were made with distilled and deionized water prepared using a Millipore Milli-RO 10 Plus and Milli-Q UF Plus at 18 M $\Omega$  resistance (Millipore, Bedford, USA). Phosphate buffered saline powder was purchased from MP Biomedicals (pH 7.4, 9.55 g/L, Solon, USA). Artificial cerebrospinal fluid (aCSF) at a pH of 7.4 was prepared as previously described [25]. All other solvents and reagents were supplied by Sigma-Aldrich and used as received.

### 2.2. Preparation of HMC hydrogels and composite hydrogels

Physical hydrogel blends of hyaluronan (HA) and methyl cellulose (MC) were prepared in the following compositions in aCSF; 2 wt.% 1700 kg/mol HA, 7 wt.% 13 kg/mol MC (2:7 HMC); 1 wt.% 2600 kg/mol HA, 3 wt.% 300 kg/mol MC (1:3 HMW HMC); 2% 2600 kg/mol HA, 3 wt.% 300 kg/mol MC (2:3 HMW HMC); and 3 wt.% 2600 kg/mol HA, 3 wt.% 300 kg/mol MC (3:3 HMW HMC). In each case MC was mechanically dispersed using a planetary mixer (Flacktek Inc., Landrum, USA) and left to dissolve overnight at 4  $^{\circ}$ C. HA was then added to the MC solution, dispersed, and dissolved in the same way. Cold solutions were centrifuged to remove entrained bubbles, resulting in transparent hydrogels.

Drug loaded hydrogels were prepared by dispersing dry drug formulations or concentrated, buffered solutions in HAMC using a planetary mixer and left to dissolve overnight at 4 °C before use. Drug loaded PLGA particles and model polystyrene particles were dispersed in HAMC immediately prior to use.

### 2.3. Rheological characterization of HAMC hydrogels

The storage and loss moduli of 2:7 HAMC and the HMW HAMC hydrogels were determined as a function of oscillation frequency on an AR-1000 rheometer fitted with a 40 mm, 2° cone and plate geometry (TA Instruments, New Castle, USA). An amplitude sweep was performed to confirm that the frequency and strain were within the linear viscoelastic region. Temperature was controlled at 37 °C using the integrated Peltier plate and sample evaporation was minimized using a solvent trap. After 5 min equilibration the frequency sweep was conducted from 0.1–100 rad/s at 12% strain for all materials.

### 2.4. In vitro stability and swelling of composite HAMC hydrogels

Approximately 150 mg of HMW HAMC loaded with 0, 25, or 75 mg/mL of 220 nm or 830 nm polystyrene nanoparticles was deposited into pre-weighed polypropylene sample tubes, weighed, warmed to 37 °C, and combined with 800 µL of warm aCSF. Samples were incubated at 37 °C on a rotary shaker at 2 Hz throughout the study and the aCSF buffer sampled with total replacement after: 1 h, 6 h, and 1, 3, 7, 14, 21, and 28 days. Recovered buffer was sonicated to disrupt residual hydrogel (Sonics, Newtown, USA) and create a uniform nanoparticle suspension. The concentration of 220 nm particles was determined by a turbidity assay at 500 nm on an Agilent 8453 spectrophotometer (Agilent Technologies, Santa Clara, USA).

The swelling ratio,  $Q$ , of HAMC and composites was determined by accurately weighing each gel sample in the stability study after the aCSF had been removed, correcting for residual buffer, and dividing by the original hydrated sample mass. To compare the degradation of composites with different swelling characteristics, normalized  $Q$  was defined as:

$$\frac{Q(t)}{Q_{max}} \quad (1)$$

where  $Q_{max}$  is the maximum recorded swelling ratio of the sample.

### 2.5. Determination of drug diffusivity in HMW HAMC

The diffusivity of a given drug in HMW HAMC,  $D$ , was normalized to its diffusivity in water,  $D_o$ , to determine the impact of HMW HAMC on molecular diffusion [30]. Approximations of  $D$  for NBQX,  $\alpha$ -chymotrypsin, and IgG in HMW HAMC were estimated according to the one dimensional, unidirectional, thin film approximation for non-swelling samples at short times [31]. Normalized diffusion coefficients were then determined with respect to previously reported values of  $D_o$  according to:

$$\frac{D}{D_o} = \frac{\pi \left( \frac{M_t}{M_\infty} \right)^2}{D_o t} \quad (2)$$

Where  $M_t/M_\infty$  is the cumulative mass of drug detected at time,  $t$ , divided by the total mass released and  $l$  is the sample thickness.

Approximately 100 mg of HAMC with a drug loading of 100–1000 µg/mL was deposited into a cylindrical sample tube to yield a gel with thickness of 0.3 cm and one exposed surface. Samples were warmed to 37 °C and combined with 900 µL of warm aCSF. The buffer was sampled with total replacement at 0.5, 1, 2, and 5 h and analyzed as described in Section 2.6.

### 2.6. Drug release from HAMC hydrogels

Release profiles of each particle encapsulated drug were obtained by depositing approximately 150 mg of drug loaded 2:3 HMW HAMC into polypropylene sample tubes, warming to 37 °C, and adding 600 µL warm aCSF. Samples were incubated at 37 °C on a rotary shaker at 2 Hz throughout the study and the aCSF buffer sampled with total replacement after 0.5, 1, 3, 7, 14, 21, and 28 days. Particle loads were typically 30–40 mg PLGA per gram of composite. Release profiles of dissolved drugs were obtained in the same manner with more frequent sampling, typically at 0.5, 1, 3, 6, 24, and 72 h. All sample aliquots were immediately frozen and stored at –20 °C until analysis. IgG,  $\alpha$ -chymotrypsin, and EGF concentrations were determined by the bicinchoninic acid assay (BCA) (Thermo Fisher Scientific, Rockford, USA); NBQX and dbcAMP by UV absorbance at 425 and 273 nm, respectively; and FGF-2 by ELISA (R&D Systems, Minneapolis, USA). Each sample was thawed immediately prior to assay and clear supernatant analyzed for dissolved drug.

### 2.7. Preparation and characterization of drug loaded PLGA particles

PLGA microparticle synthesis was optimized for each factor encapsulated and thus synthesis varied slightly for each factor, described below for EGF, dbcAMP, IgG and  $\alpha$ -chymotrypsin. Microparticle size was determined by laser diffraction (Mastersizer 2000, Malvern Instruments, Malvern, UK): nanoparticle size was determined by dynamic light scattering (Zetasizer Nano ZS, Malvern Instruments). Encapsulation efficiency was defined as the fraction of drug detected per unit mass of particle compared to the theoretical maximum. Particle yield is the mass of recovered particulate PLGA adjusted for drug content, divided by the initial PLGA mass. Drug loading is the mass fraction of drug in the particles expressed as microgram of drug per milligram of particles.

#### 2.7.1. Preparation of EGF loaded PLGA microparticles

EGF loaded microparticles were prepared by a water–oil–water double emulsion (w/o/w) method with an inner aqueous phase of 100 µL, 20 mg/mL EGF in PBS, an organic phase of 1.5 mL, 100 mg/mL PLGA (0.15–0.25 dL/g) in DCM and an outer aqueous phase of 50 mL, 10 mg/mL PVA and 100 mg/mL NaCl. The primary emulsion was created by 10 s of vortexing (Scientific Industries, Bohemia, USA) followed by 15 s of sonication. The secondary emulsion was formed by addition of the outer aqueous phase and homogenization by a Kinematica PT3000 (Brinkmann, Mississauga, CA). The double emulsion was then added to 150 mL of a 100 mg/mL NaCl and 1 mg/mL PVA solution and stirred for 4 h at room temperature. EGF loaded PLGA microparticles were isolated and washed 4 times by centrifugation, lyophilized, irradiated with 2.5 kGy gamma rays, and stored at –20 °C.

EGF content was determined by degrading the PLGA in 1 M NaOH for 24 h at 37 °C, centrifuging the resulting suspension and assaying the supernatant for total protein using the BCA assay.

#### 2.7.2. Preparation of dbcAMP loaded PLGA microparticles

dbcAMP loaded microparticles were prepared from a w/o/w double emulsion, with an inner aqueous phase of 75 µL, 267 mg/mL dbcAMP in ddH<sub>2</sub>O, an organic phase of 600 µL, 217 mg/mL PLGA (0.20 dL/g) in a 75:25 v/v solution of DCM and acetone, and an outer aqueous phase of 25 mL, 25 mg/mL PVA and 100 mg/mL NaCl. The primary and secondary emulsions were created by 45 s of sonication and homogenization, respectively. The double emulsion was then added to 200 mL of a 100 mg/mL NaCl and 2.5 mg/mL PVA solution and stirred for 3 h at room temperature. dbcAMP loaded PLGA microparticles were isolated and washed with ddH<sub>2</sub>O over a 200 nm nylon filter, lyophilized, irradiated with 2.5 kGy gamma rays, and stored at –20 °C.

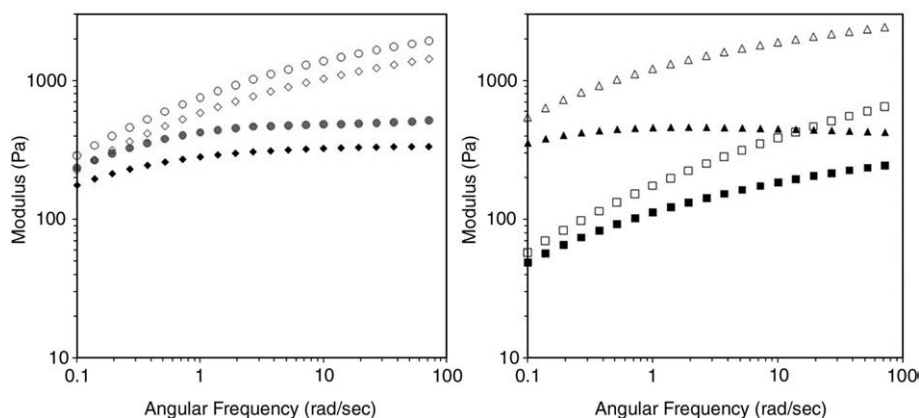


**Fig. 2.** Storage ( $G'$ , open symbols) and loss modulus ( $G''$ , filled symbols) of injectable gels. 2:3 HMW HMC ( $\diamond$ ) and 2:7 HMC ( $\circ$ ) are gels and behave similarly at low frequencies (left). 1:3 HMW HMC ( $\square$ ) and 3:3 HMW HMC ( $\Delta$ ) are shown on the right.

dbcAMP content was determined by DCM/water solvent extraction. PLGA was dissolved in DCM and extracted 3 $\times$ . Aqueous dbcAMP concentration was determined by UV absorbance at 273 nm on a Nanodrop ND-1000 (Thermo Fisher Scientific).

### 2.7.3. Preparation of IgG and $\alpha$ -chymotrypsin loaded PLGA nanoparticles

IgG loaded nanoparticles were prepared from a w/o/w double emulsion, with an inner aqueous phase of 100  $\mu$ L, 10 mg/mL IgG in aCSF, an organic phase of 0.9 mL, 50 mg/mL PLGA (0.15–0.25 dL/g) and 0.5 mg/mL Pluronic F-127 in DCM, and an outer aqueous phase of 3 mL, 25 mg/mL PVA. The primary emulsion was created by 10 min of sonication over ice. The secondary emulsion was formed by addition of the outer aqueous phase and sonication for a further 10 min over ice. The double emulsion was then added to 40 mL of a 25 mg/mL PVA solution and stirred for 20 h at room temperature.  $\alpha$ -Chymotrypsin loaded nanoparticles were produced in an identical manner with the addition of 1 mg/mL of DCM to the final aqueous volume prior to combination with the double emulsion. Protein loaded PLGA nanoparticles were isolated and washed 4 times by ultracentrifugation, lyophilized, and stored at  $-20$   $^{\circ}$ C.

Protein content was determined based on a method by Wong et al. [32]. Briefly, nanoparticles were dissolved in DMSO at 37  $^{\circ}$ C and then diluted with 50 mM NaOH. The resulting suspension was allowed to settle and the supernatant assayed for total protein using the BCA assay.

### 2.8. Statistical analysis

Data are expressed as means  $\pm$  standard deviation unless otherwise noted. Comparisons of groups of means were determined by ANOVA and pairs of mean by Student's  $t$ -test where appropriate. Significance was assigned at  $p < 0.05$ .

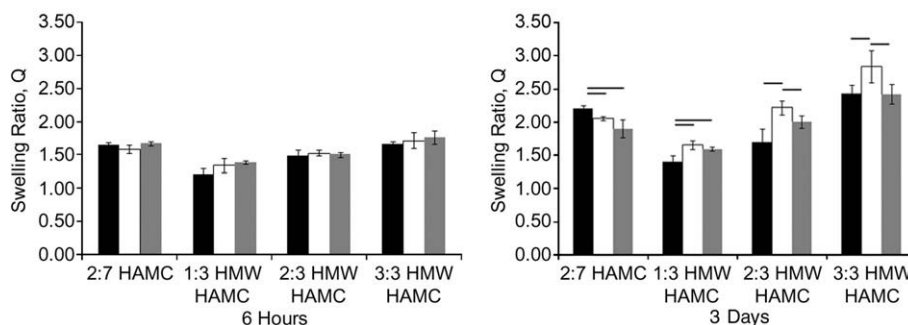


**Fig. 3.** Each of the HMW HMC formulations swell similarly or less than 2:7 HMC after 6 h. All materials reached a maximum swelling ratio at 3 days. The traces are; 0 mg/mL ( $\blacksquare$ ), 25 mg/mL ( $\square$ ), and 75 mg/mL ( $\blacksquare$ ) of 220 nm polystyrene particles dispersed in the hydrogel.

## 3. Results and discussion

### 3.1. Rheology of hyaluronan and methyl cellulose hydrogels

While previous 2:7 HMC formulations degraded *in vivo* within 4–7 days [28], the goal here was to develop a more stable HMC for longer term delivery while maintaining the properties of injectability and fast gelation. We hypothesized that higher molecular weight HA and MC would provide enhanced stability. Blends of 1–3% HA (2600 kg/mol) and 3% MC (300 kg/mol) met our qualitative criteria of fast gelation and injectability through a 30G/200  $\mu$ m inner diameter needle and were compared to 2:7 HMC by rheology. The frequency sweeps shown in Fig. 2 were conducted at 37  $^{\circ}$ C and revealed the new compositions were of a similar stiffness to 2:7 HMC and that 2:3 HMW HMC was most like the original hydrogel. This observation was of practical importance because the stiffness of 2:7 HMC approached the upper limit of what can be injected in the intrathecal space using the method described by Jimenez-Hamann et al. [21].

### 3.2. Hydrogel swelling and degradation

As a cross-linked hydrogel containing the polyelectrolyte HA, HMC swells when placed in a reservoir of aCSF *in vitro* or CSF *in vivo*. It is possible that an intrathecally injected hydrogel, resting between the pia and arachnoid mater, may put pressure on the spinal cord as the material swells in CSF. The swelling ratio,  $Q$ , at early times and maximal swelling ratio,  $Q_{max}$ , are both of interest because the spinal cord can tolerate larger gel volumes if the swelling force is progressively applied over longer periods [33]. We previously demonstrated that injections of 20  $\mu$ L of collagen gel or 10  $\mu$ L of 2:7 HMC were safe in a rat model of SCI [25,28]. Although the maximum

safe gel volume *in vivo* is not well characterized, the 2:7 HMC formulation reached a maximum swelling ratio,  $Q_{\max}$ , of 2.2 at 3 days *in vitro* and was shown to be safe *in vivo*, suggesting that this value is acceptable. By comparison, at three days the  $Q_{\max}$  for 1:3 HMW HMC was 1.4 and 2:3 HMW HMC was 1.8 whereas 3:3 HMW HMC was 2.4, nominally higher than 2:7 HMC. The increase in  $Q_{\max}$  as a function of HA concentration reflects an increase in osmotic pressure common to polyelectrolytes [34]. Swelling at early times, shown at 6 h in Fig. 3, was similarly comparable between 2:7 HMC and the HMW HMC blends. The three HMW HMC formulations met our swelling criteria, permitting an *in vivo* injection volume of  $\sim 10 \mu\text{L}$  and maximum gel volume similar to 2:7 HMC over time.

As the first step toward composite drug delivery the swelling behaviour of HMC composites was determined at particle loads of 25 and 75 mg/mL, and particle diameters of 220 and 830 nm. Polystyrene (PS) particles were used as model hydrophobic polymer beads to simulate PLGA microspheres because of their narrow size distribution and range of available diameters. No difference in swelling was observed as a function of particle diameter for any HMC formulation at any loading (data not shown). As shown in Fig. 3 for 220 nm particles dispersed in various HMC hydrogels, these formulations with nanoparticles reached maximum swelling on day 3, at which time an effect of particle loading on swelling became significant.

The swelling behaviour of the composites can be partially explained if the particles are considered as non-interacting spheres which increase the volume fraction of polymer,  $\nu_{2,s}$ , in the gel by displacing aCSF. According to the Peppas–Merrill equation of hydrogel swelling,  $Q$  decreases as  $\nu_{2,s}$  is increased [35]. For example, a 75 mg/mL particle load increases the aqueous MC content in HMW HMC from 3.0% to 3.2% by displacing aCSF. This mechanism accounts for the reduced swelling in HMW HMC when particle loading was increased from 25 to 75 mg/mL for all blends, and why  $Q$  is independent of particle diameter, since only the total mass of buffer displaced is considered. It does not, however, account for the increase in  $Q$  from zero to 25 mg/mL particles in each HMW HMC. This unexpected increase in swelling may be a kinetic effect not well described by equilibrium swelling theory. Importantly, both 1:3 and 2:3 HMW HMC at 25 and 75 mg/mL swelled similarly to, or less than, our pre-existing drug delivery system, supporting the safety of these materials *in vivo*.

We followed the *in vitro* degradation of the three HMW HMC blends with and without PS particles by measuring the swelling ratio over time relative to  $Q_{\max}$ . For the HMW HMC swelling traces in Fig. 4, 1:3 HMW HMC was most stable, followed by 2:3 and 3:3 HMW HMC. Since HMC gels through physical cross-links between methyl cellulose, the higher concentration of MC in the minimally swollen gels results in slower degradation. This is supported by Peppas and Merrill who showed that lower swelling ratios are the result of more physical cross-links and are therefore predictive of slower degradation/dissolution [35].

Dispersing nanoparticles in all HMW HMC resulted in significantly slower degradation regardless of particle loading (25 or 75 mg/mL) or diameter (220 or 830 nm). For 1:3 HMW HMC, inclusion of nanoparticles resulted in gels that retained 80% of  $Q_{\max}$  at 28 days relative to gels alone that retained only 60% of  $Q_{\max}$ . For 2:3 and 3:3 HMW HMC, dispersing hydrophobic nanoparticles stabilized the gel and left a majority of the composite intact when the blank hydrogels had completely degraded. For 2:3 HMW HMC, which had degraded completely by 28 days, inclusion of nanoparticle resulted in 70–80% retention of  $Q_{\max}$ . For 3:3 HMW HMC, which had completely degraded at 21 days, the inclusion of particles resulted in 60–80% retention of  $Q_{\max}$  then, and 30–60% at 28 days. As with initial swelling, particle diameter did not measurably affect degradation. Based on previously observed differences between HMC degradation *in vitro* and *in vivo*, where 2:7 HMC was observed to degrade faster after intrathecal injection [28], it was desirable that the new drug delivery

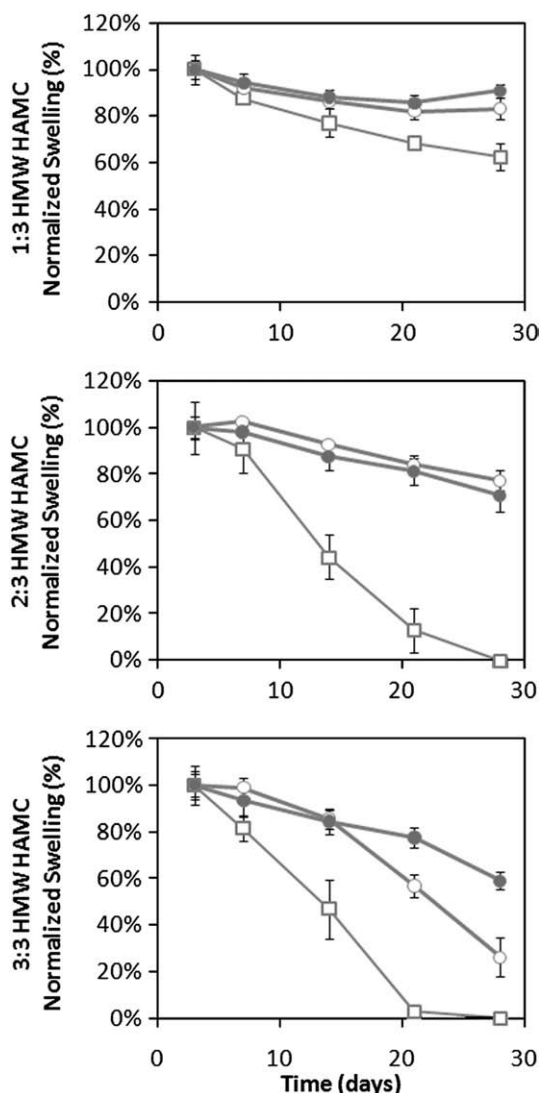


Fig. 4. The degradation of HMW HMC and composite HMW HMC was quantified by the swelling ratio and represented as change in composite volume relative to  $Q_{\max}$ . Degradation of HMW HMC (□) was faster than composite HMW HMC of the same formulation in all cases. No significant effect of particle diameter on degradation was found. Open circles are 25 mg/mL of 220 nm particles (○), and filled circles are 75 mg/mL (●).

platform remain substantially intact at 28 days *in vitro*. 1:3 HMW HMC met this criterion under all conditions and 2:3 HMW HMC was satisfactory in the presence of nanoparticles.

The residual particle load was quantified for the 220 nm particle loaded composites as a direct measure of the composite's utility as a drug delivery platform. The residual particle load, defined as the mass of particles in the gel at time,  $t$ , divided by the initial particle mass, was followed by injecting 150 mg of nanoparticle loaded hydrogel in 800  $\mu\text{L}$  of aCSF. Substantial numbers of the 220 nm and larger particles were not predicted to diffuse from the composite in the absence of HMW HMC degradation because the particles were significantly larger than the mesh sizes typically reported for hydrogels [36]. In Fig. 5, a small release of less than 2% of nanoparticles was seen from each of the composites in the hours after injection, followed by a delay in particle loss as the composites shrank with the reorganization of the MC hydrophobic network and formation of optimized cross-links [26]. At 28 days the residual particle load was 40% for 3:3 HMW HMC, 84% for 2:3 HMW HMC and 98% for 1:3 HMW HMC, following the degradation pattern of the hydrogels. Residual particle loads were not dependent on initial mass loading (25 or 75 mg/mL)

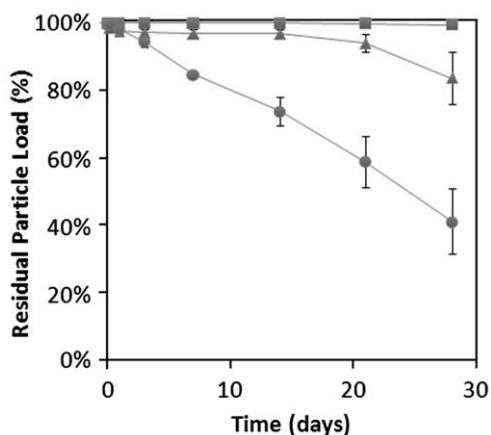


Fig. 5. The loss of particles from composite HMW HAMC was a strong function of gel composition. The traces are: 1:3 HMW HAMC (■), 2:3 HMW HAMC (▲), 3:3 HMW HAMC (●), each loaded with 25 mg/mL of 220 nm PS particles.

after 28 days. These results were consistent with the characterization of 1:3 HMW HAMC as having the lowest swelling ratio, greatest stability, highest weight fraction of MC, and lowest predicted molecular weight between cross-links.

The mechanism of nanoparticle mediated stabilization remains unclear, although one possibility is based on network optimization [26], supported by the reduction in normalized swelling without loss of embedded particles in 1:3 HMW HAMC over 28 days and 2:3 HMW HAMC over 14 days. Considering dynamic association of MC chains, those near the surface of the gel have fewer neighbouring hydrophobic regions and are likely lost from the gel by diffusion. Dispersed hydrophobic particles may slow this process by associating with MC [37], slowing diffusion and resulting in a higher fraction of MC chains re-forming hydrophobic junctions and stabilizing the composite.

To study the possible effect of embedded particles on the mechanical properties of HMW HAMC we tested the injectability of composite HMW HAMC through a 30G needle from a Hamilton 250  $\mu$ L glass syringe. Surfactant free suspensions of low polydispersity PS particles ranging from 60 nm to 15.5  $\mu$ m in diameter were lyophilized, added dry to each of the hydrogels up to 150 mg/mL, and mechanically dispersed. Given the inherent stiffness of HMW HAMC and the reported difficulty in evenly suspending hydrophobic particles in hydrogels [38,39], we expected large diameter and higher weight percent formulations would not be injectable due to incomplete dispersion and occlusion of the needle by particle aggregates. Surprisingly, each formulation was injectable at room temperature. The injection of higher concentrations and larger diameter particles enhances the utility of the drug delivery platform by both increasing the deliverable drug load and capturing the distinct release profiles reported for PLGA particles of different diameters [40,41].

### 3.3. Drug diffusivity in hydrogels

We next examined the diffusion of two high molecular weight proteins, IgG (150 kg/mol) and  $\alpha$ -chymotrypsin (25 kg/mol), from HMW HAMC since they were most likely to be restricted by sieving effects [42]. It was desirable that the normalized diffusion coefficient,  $D/D_0$ , be sufficiently large that the rate limiting step in release of particle encapsulated drugs was not diffusion through the gel. In this manner long-term drug release is controlled by the particle formulation and the release profile is decoupled from molecular diffusivity. Plotting the fractional release of IgG and  $\alpha$ -chymotrypsin against  $t^{1/2}$  yielded a linear relationship, as predicted for Fickian diffusion [43]. Applying a  $D_0$  of  $6.4 \times 10^{-7}$   $\text{cm}^2/\text{s}$  for IgG [44] and an estimated  $D_0$  of  $1.5 \times 10^{-6}$   $\text{cm}^2/\text{s}$  for  $\alpha$ -chymotrypsin [45], the normalized diffusion coefficient of IgG ranged from 0.04 in 3:3 HMW HAMC to 0.25 in 1:3

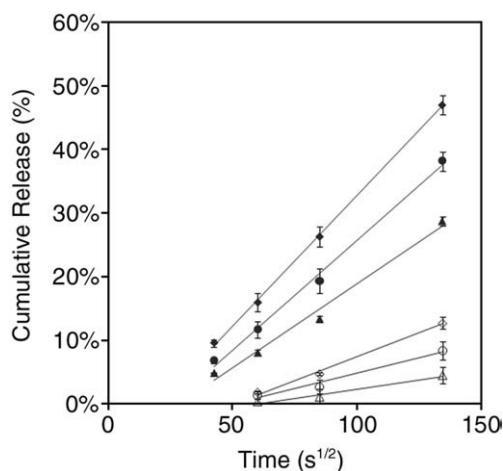


Fig. 6. The slope of IgG and  $\alpha$ -chymotrypsin release from HMW HAMC decreases as HA concentration increases, indicating HA slowed diffusion.  $D/D_0$  was lowest for both molecules in 3:3 HMW HAMC, on the order of 0.3 and 0.04 for  $\alpha$ -chymotrypsin and IgG, respectively. The non-zero intercept indicates that swelling has slowed drug release, reducing  $D$ . The traces are: 1:3 HMW HAMC ( $\diamond$ ), 2:3 HMW HAMC ( $\circ$ ), and 3:3 HMW HAMC ( $\triangle$ ).  $\alpha$ -Chymotrypsin release is represented by filled symbols and IgG release by open symbols.

HMW HAMC and  $\alpha$ -chymotrypsin ranged from  $\sim 0.3$  to  $\sim 0.8$  in the same materials. It is clear from the non-zero intercept in Fig. 6 that swelling impacted drug release at these early times as penetration of aCSF into the gel retards drug release. This result was expected given that for all gels within 3 h  $Q$  for all gels exceeded 1.25, the ratio above which swelling is a significant factor in drug release [46], and reduced the calculated value of  $D$ . Our *in vitro* estimation of  $D$  is therefore smaller than what can be expected *in vivo* where the restrictive environment may prevent the gel from swelling more than 1.25 $\times$  normal to the spinal cord. Both IgG and  $\alpha$ -chymotrypsin diffuse from HMW HAMC relatively quickly and release is predicted to be complete within 24 h based on the planar geometry of the gels after injection *in vivo*. This rate was advantageous, being slow enough to allow prolonged release of dissolved molecules yet fast enough that release of PLGA encapsulated molecules was not expected to be diffusion limited.

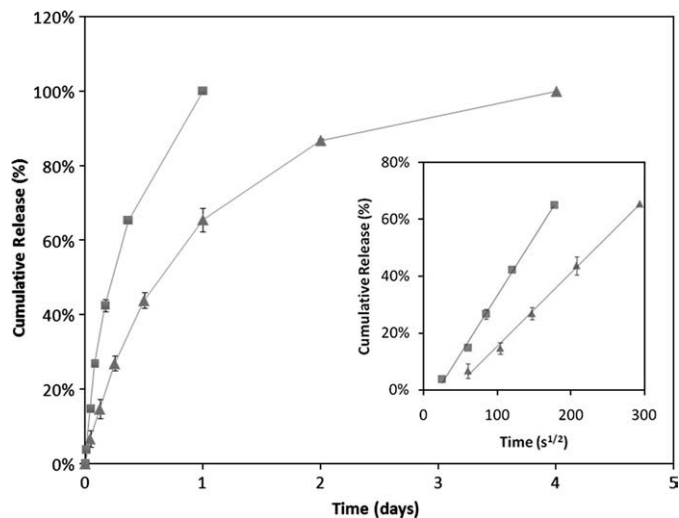
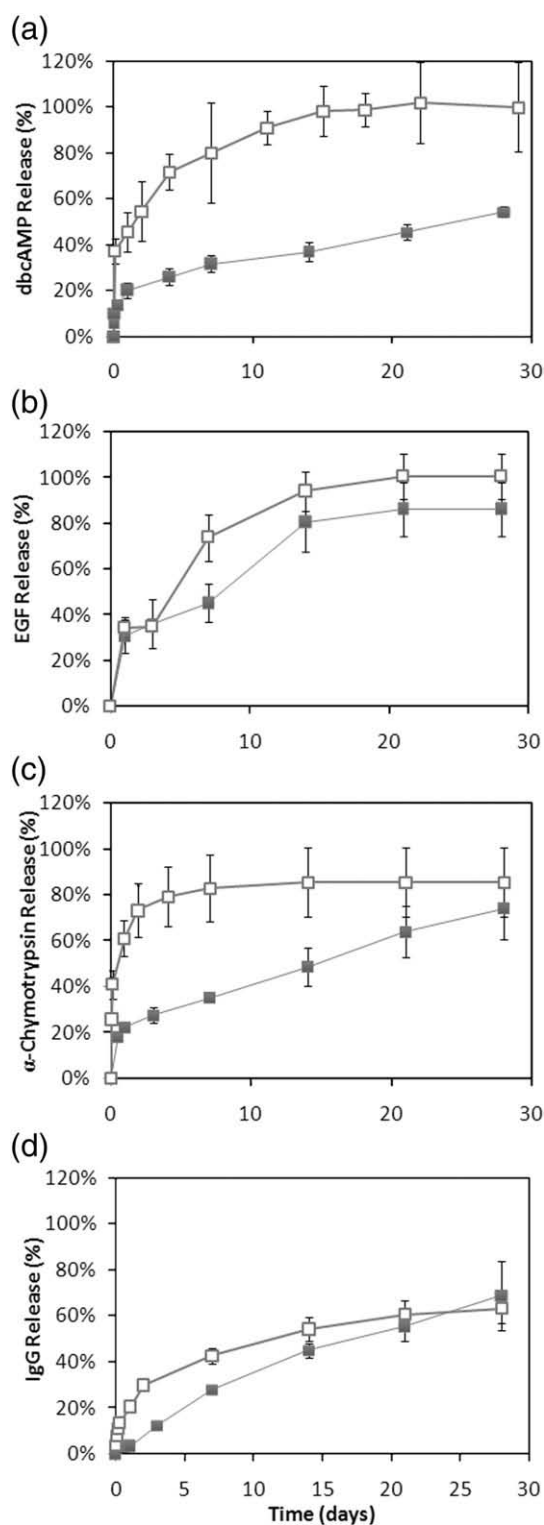


Fig. 7. The *in vitro* release of dissolved NBQX (■) and FGF-2 (▲) from 2:3 HMW HAMC is diffusion limited (inset) and complete within 1 and 4 days, respectively (main graph). Fractional release normalized to the total initial drug mass for NBQX and to total detectable protein for FGF-2.

### 3.4. Drug release from composite hydrogels

After establishing that both 1:3 and 2:3 HMW HAMC composites met our *in vitro* design criteria we followed the release of six therapeutic molecules from 2:3 HMW HAMC, chosen because the HA



**Fig. 8.** Cumulative release normalized to the amount encapsulated in the particles. The open symbols indicate release from free particles for (a) dbcAMP, (b) EGF, (c)  $\alpha$ -chymotrypsin, (d) IgG, and filled symbols from composite 2:3 HMW HAMC. The release of individual drugs from particles dispersed in 2:3 HMW HAMC is longer than from the corresponding particles alone.

**Table 2**  
Synthesis of drug loaded PLGA particles.

Molecule	Molecular weight (kg/mol)	Encapsulation efficiency (%)	Drug loading ( $\mu\text{g}/\text{mg}$ )	Particle yield (%)	Particle size ( $\mu\text{m}$ )
dbcAMP	0.469	51	68	50	$37 \pm 14$
EGF	6.2	36	4.8	63	$10 \pm 2$
$\alpha$ -Chymotrypsin	25	32	7	53	0.285, polydisperse
IgG	150	56	14	61	$0.272 \pm 0.103$

content matched 2:7 HAMC and is likely an important component in HAMC's anti-inflammatory action. NBQX and FGF-2 have been shown to play a role in neuroprotection and thus fast release from the hydrogel was desirable. Both molecules were released in a diffusion limited manner from 2:3 HMW HAMC, shown in the inset of Fig. 7, with a normalized diffusion coefficient on the order of 0.1. The release profiles, also plotted versus linear time in Fig. 7 for ease of comparison to particle mediated release in Fig. 8, show that NBQX is released from the hydrogel faster than FGF-2. The diffusive release *in vitro* is likely slower than that *in vivo*, where the release rate is bounded by fast unidirectional diffusion from a thin film [31] and the slow diffusion of many molecules through tissue [28,29,47].

Four neuroregenerative molecules (or models thereof) were encapsulated in formulations of PLGA particles and individually dispersed in 2:3 HMW HAMC for long term release. Encapsulation in PLGA particles is widely used to control temporal drug release. In these systems the release profile results from drug diffusion through pores in the polymer matrix formed by dissolution of entrapped protein and degradation of PLGA [40,41,48]. The data for the encapsulation of dbcAMP, EGF,  $\alpha$ -chymotrypsin, and IgG are summarized in Table 2 and the drug release profiles from free particles are reported in Fig. 8.

As shown in Fig. 8, extended release over 28 days was achieved for these formulations. In a majority of these trials, the initial burst release characteristic of PLGA particles [40,41] was reduced and subsequent release was typically more linear and longer from PLGA particles dispersed in HMW HAMC composite gels than from the particles alone. This observation was in agreement with the work of Ying et al. [49], although in the current case only a small portion of the effect was due to molecular diffusion through the gel. In HMW HAMC diffusion can only prolong release for 1–4 days after release from the particle, as reported in Fig. 6 for IgG and  $\alpha$ -chymotrypsin and in Fig. 7 for NBQX and FGF-2. Visual observation of particle loaded composites, which remained opaque during these experiments, suggests decreased degradation of PLGA particles dispersed in HMW HAMC relative to particles dispersed in aqueous buffer. In each case the particles, which scatter light and cause the composite to appear opaque and white, remained intact. If the PLGA were hydrolyzed at the rate reported for free particles [48], opacity would have decreased over time as particle size and number were reduced. If instead the rate of PLGA degradation was reduced in the composite, drug release would be slower than from particles alone and the composites would remain opaque as observed. This may be the result of MC adsorption onto the particle surface [37], resulting in slower diffusion of drug and degraded PLGA through pores in the polymer matrix, mechanisms supported by the reduction in burst release observed for dbcAMP,  $\alpha$ -chymotrypsin, and IgG. A MC/particle interaction is also supported by the increase in HMW HAMC stability on particle addition, discussed in Section 3.2. The atypical behaviour of the EGF loaded particles may indicate more of the drug is near the particle surface and less subject to variation in PLGA degradation.

As an injectable drug delivery platform, the particle loaded hydrogels allow different drug formulations to be dispersed within the hydrogel to create a combination therapy while maintaining

control of the resulting release profiles. Existing drug and particle formulations can be directly dispersed in the hydrogel without modification, and the combination of fast diffusion limited release from the dissolved phase and slow release of particle-borne drugs can be exploited such that release can be substantially decoupled from molecular weight. We have shown the *in vitro* release of the small molecules NBQX and dbcAMP over 1 and 28 days, respectively, and the release of proteins spanning 6–150 kg/mol over 4–28 days. Particle loads up to 15 wt.% were injectable, resulting in a deliverable drug load of 1.1–10.1 mg per gram of composite as a function of PLGA particle properties. The 2:3 HMW HAMC used to evaluate drug release retained greater than 80% of the initial particle load after 28 days, suggesting that a high percentage of the drug loaded will be locally delivered at the site of injection.

#### 4. Conclusion

Our work is directed toward the development of a clinically acceptable drug delivery platform for the treatment of spinal cord injury. In this report we described the development of a series of physical hydrogels composed of hyaluronan and methyl cellulose and demonstrated that these materials met the design criteria of injectability, safe swelling, satisfactory diffusivity of molecules up to 150 kg/mol, high residual particle load, and significantly slower *in vitro* degradation relative to earlier reports. The slow degradation rate of HMW HAMC with particles dispersed therein suggests this as a platform for 28 day combination drug therapy. We demonstrated that composites with particle loads up to 15 wt.% and 0.06–15.5  $\mu\text{m}$  diameter remained injectable for all blends and that greater than 95% of the initial particle load was retained after 28 days *in vitro* in 1:3 HMW HAMC. Utilizing a combination of diffusion limited and particle mediated drug delivery, we showed release of six neuroprotective and neuroregenerative drugs from 1 to 28 days. On the basis of these data, composite HMW HAMC is a promising intrathecal drug delivery platform which affords independent, flexible delivery of one or more drugs over 28 days. We are currently evaluating the safety and degradation behaviour of these materials in a rat model of spinal cord injury.

#### Acknowledgment

We are grateful to CIHR MOP# 44054 for funding (MSS). MDB, JCS, and YW acknowledge NSERC for CGSD, USRA, and PGSM scholarships, respectively. YL acknowledges a McEwen Fellowship.

#### References

- [1] J. Wosnick, M.D. Baumann, M.S. Shoichet, in: A. Atala, R. Lanza, J.A. Thomson, R.M. Nerem (Eds.), *Tissue therapy in the central nervous system, in principles of regenerative medicine*, Elsevier, New York, 2007.
- [2] S.M. Miller, Methylprednisolone in acute spinal cord injury: a tarnished standard, *J. Neurosurg. Anesthesiol.* 20 (2) (2008) 140–142.
- [3] I. Rozet, Methylprednisolone in acute spinal cord injury: is there any other ethical choice? *J. Neurosurg. Anesthesiol.* 20 (2) (2008) 137–139.
- [4] L.M. Ramer, M.S. Ramer, J.D. Steeves, Setting the stage for functional repair of spinal cord injuries: a cast of thousands, *Spinal Cord* 43 (3) (2005) 134–161.
- [5] M.B. Bracken, et al., Methylprednisolone or naloxone treatment after acute spinal cord injury: 1-year follow-up data. Results of the second National Acute Spinal Cord Injury Study, *J. Neurosurg.* 76 (1) (1992) 23–31.
- [6] Y. Li, et al., Effects of the AMPA receptor antagonist NBQX on the development and expression of behavioral sensitization to cocaine and amphetamine, *Psychopharmacology (Berl)* 134 (3) (1997) 266–276.
- [7] A. Scriabine, T. Schuurman, J. Traber, Pharmacological basis for the use of nimodipine in central nervous system disorders, *Faseb J.* 3 (7) (1989) 1799–1806.
- [8] M.I. Romero, et al., Functional regeneration of chronically injured sensory afferents into adult spinal cord after neurotrophin gene therapy, *J. Neurosci.* 21 (21) (2001) 8408–8416.
- [9] C.A. Tobias, et al., Delayed grafting of BDNF and NT-3 producing fibroblasts into the injured spinal cord stimulates sprouting, partially rescues axotomized red nucleus neurons from loss and atrophy, and provides limited regeneration, *Exp. Neurol.* 184 (1) (2003) 97–113.
- [10] D.L. Kitchens, E.Y. Snyder, D.I. Gottlieb, FGF and EGF are mitogens for immortalized neural progenitors, *J. Neurobiol.* 25 (7) (1994) 797–807.
- [11] A. Bikfalvi, et al., Biological roles of fibroblast growth factor-2, *Endocr. Rev.* 18 (1) (1997) 26–45.
- [12] T.T. Lee, et al., Neuroprotective effects of basic fibroblast growth factor following spinal cord contusion injury in the rat, *J. Neurotrauma* 16 (5) (1999) 347–356.
- [13] Y.D. Teng, et al., Basic fibroblast growth factor increases long-term survival of spinal motor neurons and improves respiratory function after experimental spinal cord injury, *J. Neurosci.* 19 (16) (1999) 7037–7047.
- [14] D.N. Loy, et al., Temporal progression of angiogenesis and basal lamina deposition after contusive spinal cord injury in the adult rat, *J. Comp. Neurol.* 445 (4) (2002) 308–324.
- [15] M.E. Schwab, Nogo and axon regeneration, *Curr. Opin. Neurobiol.* 14 (1) (2004) 118–124.
- [16] L. McKerracher, H. Higuchi, Targeting Rho to stimulate repair after spinal cord injury, *J. Neurotrauma* 23 (3–4) (2006) 309–317.
- [17] S.S. Hannila, M.T. Filbin, The role of cyclic AMP signaling in promoting axonal regeneration after spinal cord injury, *Exp. Neurol.* 209 (2) (2008) 321–332.
- [18] H. Terada, et al., Reduction of ischemic spinal cord injury by dextrorphan: comparison of several methods of administration, *J. Thorac Cardiovasc. Surg.* 122 (5) (2001) 979–985.
- [19] T.L. Yaksh, et al., Intrathecal ketorolac in dogs and rats, *Toxicol. Sci.* 80 (2) (2004) 322–334.
- [20] L.L. Jones, M.H. Tuszynski, Chronic intrathecal infusions after spinal cord injury cause scarring and compression, *Microsc. Res. Tech.* 54 (5) (2001) 317–324.
- [21] M.C. Jimenez Hamann, et al., Novel intrathecal delivery system for treatment of spinal cord injury, *Exp. Neurol.* 182 (2) (2003) 300–309.
- [22] S.A. Chvatal, et al., Spatial distribution and acute anti-inflammatory effects of Methylprednisolone after sustained local delivery to the contused spinal cord, *Biomaterials* 29 (12) (2008) 1967–1975.
- [23] C.H. Tator, et al., Current use and timing of spinal surgery for management of acute spinal surgery for management of acute spinal cord injury in North America: results of a retrospective multicenter study, *J. Neurosurg.* 91 (1 Suppl) (1999) 12–18.
- [24] M.G. Fehlings, C.H. Tator, An evidence-based review of decompressive surgery in acute spinal cord injury: rationale, indications, and timing based on experimental and clinical studies, *J. Neurosurg.* 91 (1 Suppl) (1999) 1–11.
- [25] D. Gupta, C.H. Tator, M.S. Shoichet, Fast-gelling injectable blend of hyaluronan and methylcellulose for intrathecal, localized delivery to the injured spinal cord, *Biomaterials* 27 (11) (2006) 2370–2379.
- [26] N. Schuppper, Y. Rabin, M. Rosenbluh, Multiple stages in the aging of a physical polymer gel, *Macromolecules* 41 (11) (2008) 3983–3994.
- [27] D. Jiang, J. Liang, P.W. Noble, Hyaluronan in tissue injury and repair, *Annu. Rev. Cell Dev. Biol.* 23 (2007) 435–461.
- [28] C.E. Kang, et al., A new paradigm for local and sustained release of therapeutic molecules to the injured spinal cord for neuroprotection and tissue repair, *Tissue Eng Part A* 15 (3) (2009) 595–604.
- [29] M.C. Jimenez Hamann, C.H. Tator, M.S. Shoichet, Injectable intrathecal delivery system for localized administration of EGF and FGF-2 to the injured rat spinal cord, *Exp. Neurol.* 194 (1) (2005) 106–119.
- [30] N.A. Peppas, C.T. Reinhart, Solute diffusion in swollen membranes.1. A new theory, *J. Membr. Sci.* 15 (3) (1983) 275–287.
- [31] J. Crank, *The Mathematics of Diffusion*, Clarendon Press, Oxford, 1956.
- [32] H.M. Wong, J.J. Wang, C. Wang, In vitro sustained release of human immunoglobulin G from biodegradable microspheres, *Ind. Eng. Chem. Res.* 40 (2001) 933–948.
- [33] K. Uchida, et al., Progressive changes in neurofilament proteins and growth-associated protein-43 immunoreactivities at the site of cervical spinal cord compression in spinal hyperostotic mice, *Spine* 27 (5) (2002) 480–486.
- [34] B. Gerdin, R. Hallgren, Dynamic role of hyaluronan (HYA) in connective tissue activation and inflammation, *J. Int. Med.* 242 (1) (1997) 49–55.
- [35] N.A. Peppas, E.W. Merrill, Poly(vinyl-alcohol) hydrogels – reinforcement of radiation-crosslinked networks by crystallization, *J. Polym. Sci. Part a-Polym. Chem.* 14 (2) (1976) 441–457.
- [36] C.C. Lin, A.T. Metters, Hydrogels in controlled release formulations: network design and mathematical modeling, *Adv. Drug Deliv. Rev.* 58 (12–13) (2006) 1379–1408.
- [37] F.L. Saunders, Adsorption of methylcellulose on polystyrene latexes, *J. Colloid Interface Sci.* 28 (3–4) (1968) 475–8.
- [38] X. Liu, K. Nakamura, A.M. Lowman, Composite hydrogels for sustained release of therapeutic agents, *Soft Materials* 1 (3) (2003) 393–408.
- [39] M.E. Mackay, et al., General strategies for nanoparticle dispersion, *Science* 311 (5768) (2006) 1740–1743.
- [40] V.R. Sinha, A. Trehan, Biodegradable microspheres for protein delivery, *J. Control. Release* 90 (3) (2003) 261–280.
- [41] K.S. Soppimath, et al., Biodegradable polymeric nanoparticles as drug delivery devices, *J. Control. Release* 70 (1–2) (2001) 1–20.
- [42] W.E. Hennink, et al., Controlled release of proteins from dextran hydrogels, *J. Control. Release* 39 (1) (1996) 47–55.
- [43] P.L. Ritger, N.A. Peppas, A simple equation for description of solute release 1. Fickian and non-Fickian release from non-swellable devices in the form of slabs, spheres, cylinders or discs, *J. Control. Release* 5 (1987) 23–36.
- [44] G.M. Cruise, D.S. Scharp, J.A. Hubbell, Characterization of permeability and network structure of interfacially photopolymerized poly(ethylene glycol) diacrylate hydrogels, *Biomaterials* 19 (14) (1998) 1287–1294.
- [45] J.H. Han, et al., Lactitol-based poly(ether polyol) hydrogels for controlled release chemical and drug delivery systems, *J. Agric. Food Chem.* 48 (11) (2000) 5278–5282.

- [46] P.L. Ritger, N.A. Peppas, A simple equation for description of solute release 2. Fickian and anomalous release from swellable devices, *J. Control. Release* 5 (1987) 37–42.
- [47] C.E. Krewson, M.L. Klarman, W.M. Saltzman, Distribution of nerve growth factor following direct delivery to brain interstitium, *Brain Res.* 680 (1–2) (1995) 196–206.
- [48] M. Dunne, I. Corrigan, Z. Ramtoola, Influence of particle size and dissolution conditions on the degradation properties of polylactide-co-glycolide particles, *Biomaterials* 21 (16) (2000) 1659–1668.
- [49] L. Ying, et al., In vitro evaluation of lysozyme-loaded microspheres in thermo-sensitive methylcellulose-based hydrogel, *Chin. J. Chem. Eng.* 15 (4) (2007) 566–572.